Catalysis Letters Vol. 111, Nos. 3–4, November 2006 (© 2006)
DOI: 10.1007/s10562-006-0140-9

Nano-sized crystallites of vanadyl pyrophosphate as a highly selective catalyst for *n*-butane oxidation

Yuichi Kamiya,[a,b] Naonori Ryumon,[b] Hiroyuki Imai,[b] and Toshio Okuhara[a,b,*]

[a]*Research Faculty of Environmental Earth Science, Hokkaido University, Sapporo, 060-0810, Japan*
[b]*Graduate School of Environmental Science, Hokkaido University, Sapporo, 060-0810, Japan*

Received 2 June 2006; accepted 29 August 2006

Exfoliation-reduction of $VOPO_4 \cdot 2H_2O$ in a mixed alcohol consisting of 2-butanol and ethanol, followed by the thermal treatment in the presence of *n*-butane, O_2, and He at 663 K for 300 h, produces novel nano-sized crystallites (~50 nm) of $(VO)_2P_2O_7$. The nano-sized $(VO)_2P_2O_7$ crystallites exhibit a high selectivity to maleic anhydride (~84%) for the selective oxidation of *n*-butane.

KEY WORDS: butane; $(VO)_2P_2O_7$; nano-crystallite; selective oxidation; light alkane.

1. Introduction

Vanadyl pyrophosphate, $(VO)_2P_2O_7$, is an active component in the industrial scale selective oxidation of *n*-butane to maleic anhydride (MA) [1–3]. However, the low selectivity of this catalyst for MA remains a serious problem. Therefore, there is a need to develop new, functional forms of $(VO)_2P_2O_7$ to improve this oxidation process. Since the microstructure, that is the shape and dimensions, of $(VO)_2P_2O_7$ crystallites is generally considered to be a great influence on the catalyst's performance [4–6], control over this is a promising approach to improve the catalytic performance of $(VO)_2P_2O_7$ crystallites.

Recently, it has been reported that the exfoliation of layered materials in a solvent to form nano-sheets, followed by the reconstruction of these nano-sheets, can be used to control the microstructure of solid materials [7–12]. $VOPO_4 \cdot 2H_2O$ possesses a layered structure and is capable of intercalating various molecules, such as amines, alcohols, and carboxylic acids [13–15]. We have previously succeeded in exfoliating $VOPO_4 \cdot 2H_2O$ in various alcohols, such as 2-butanol [16,17]. The subsequent reduction of the $VOPO_4$ nano-sheets by the alcohol resulted in the formation of micrometer-size $VOHPO_4 \cdot 0.5H_2O$ crystallites having dimensions of approximately 1000 nm (length) and 150 nm (thickness), while the starting $VOPO_4 \cdot 2H_2O$ crystallites were approximately 20,000 nm in length and 1100 nm in thickness. Here, we report that the exfoliation-reduction of $VOPO_4 \cdot 2H_2O$ in a mixed alcohol of 2-butanol–ethanol, followed by the thermal treatment in the presence of *n*-butane, O_2, and He at 663 K for 300 h produces separate nano-sized crystallites (~50 nm) of $(VO)_2P_2O_7$, exhibiting a high selectivity to MA (~84%) for *n*-butane oxidation.

*To whom correspondence should be addressed.
E-mail: oku@ees.hokudai.ac.jp

2. Experimental

2.1. Preparation of $VOHPO_4 \cdot 0.5H_2O$ crystallites

A mixture of V_2O_5 (24 g, Wako Pure Chem. Ind. Ltd.), aqueous 85% H_3PO_4 (223 g, Wako Pure Chem. Ind. Ltd.), and H_2O (577 cm^3) was refluxed for 16 h. The resulting precipitate was separated by filtration, washed with acetone, and dried under ambient atmosphere. The resulting yellow solid was identified as $VOPO_4 \cdot 2H_2O$ by XRD and IR.

A suspension of $VOPO_4 \cdot 2H_2O$ (2.0 g) and 2-butanol (50 cm^3, Wako Pure Chem. Ind. Ltd.) was heated stepwise with stirring at 303, 323, 343, and 363 K for 1 h at each temperature, yielding a homogeneous, yellow solution as the result of the intercalation, and exfoliation of $VOPO_4 \cdot 2H_2O$ [16]. Ethanol (14.4 cm^3, Wako Pure Chem. Ind. Ltd.) was added at room temperature to the homogeneous 2-butanol solution and the solution was refluxed for 24 h to give a blue precipitate. The precipitate was separated by centrifugation, washed with acetone and dried under ambient atmosphere. The resulting $VOHPO_4 \cdot 0.5H_2O$ solid was denoted as EP(Bu)-Et.

As a reference, a precursor was prepared by the exfoliation-reduction process of $VOPO_4 \cdot 2H_2O$ in 2-butanl (denoted EP(Bu)) [17], for which the intercalation–exfoliation of $VOPO_4 \cdot 2H_2O$ was carried out as for EP(Bu)-Et and followed by the thermal treatment of the resulting homogeneous 2-butanol solution without

adding ethanol for 24 h to lead the formation of a light blue precipitate. A conventional precursor (denoted P(OSM)), known as the organic solvent method, was also prepared using benzyl alcohol and iso-butanol [18]; a suspension of V_2O_5 (14.6 g, Wako Pure Chem. Ind. Ltd.), H_3PO_4 (16.2 g, Wako Pure Chem. Ind. Ltd.), and a mixture of *iso*-butanol (90 cm^3, Wako Pure Chem. Ind. Ltd.) and benzyl alcohol (60 cm^3, Wako Pure Chem. Ind. Ltd.) was heated with stirring at reflux temperature for 3 h.

2.2. Transformation of $VOHPO_4 \cdot 0.5H_2O$ to catalyst and catalytic oxidation of n-butane

Transformation of $VOHPO_4 \cdot 0.5H_2O$ to catalyst and the oxidation of *n*-butane were carried out at 663 K in a flow reactor (Pyrex tube, 10 mm inside diameter) with a mixture of *n*-butane (1.5 vol%), O_2 (17 vol%), and He (balance) under atmospheric pressure. The gas at the outlet of the reactor was analyzed using on-line gas chromatography. For *n*-butane and MA, an FID GC (Shimadzu GC-8A) with a Porapak QS column (3 mm×1 m) was used. A high speed GC (Aera M200) with Porapak Q and Molecular Sieve 5A columns was utilized for the analysis of CO, CO_2, and O_2 in the gas-phase. Since the conversion and selectivity gradually changed over time, the conversion dependencies were measured by changing the total flow rate after stationary conversion and selectivity were reached, which occurred after the reaction had proceeded for 300 h.

2.3. Characterization

XRD patterns were measured by an XRD diffractometer (Miniflex, Rigaku) with CuK_α radiation. Scanning electron microscope (SEM) images were taken with an FE-SEM S-4800 (Hitachi). Transmission electron micrographs (TEM) were measured using Hitachi TEM HD 2000.

The average oxidation number of V in the sample bulk was determined by redox-titration using $KMnO_4$ and that at the surface was estimated by X-ray photoelectron spectra (XPS) obtained using a Shimadzu XPS-7000 with MgK_α radiation. The adsorption–desorption isotherms of nitrogen were measured at 77 K by an automatic adsorption apparatus (BELSORP 28SA, BEL Japan Inc.) after the catalysts were evacuated at 523 K. Specific surface area and mesopore size distributions were calculated by the BET and DH methods, respectively.

3. Results and discussion

Figure 1 shows scanning electron microscope (SEM) images of $VOHPO_4 \cdot 0.5H_2O$ prepared by the exfoliation-reduction process of $VOPO_4 \cdot 2H_2O$ in the mixture of 2-butanol and ethanol (EP(Bu)-Et), and in 2-butanol

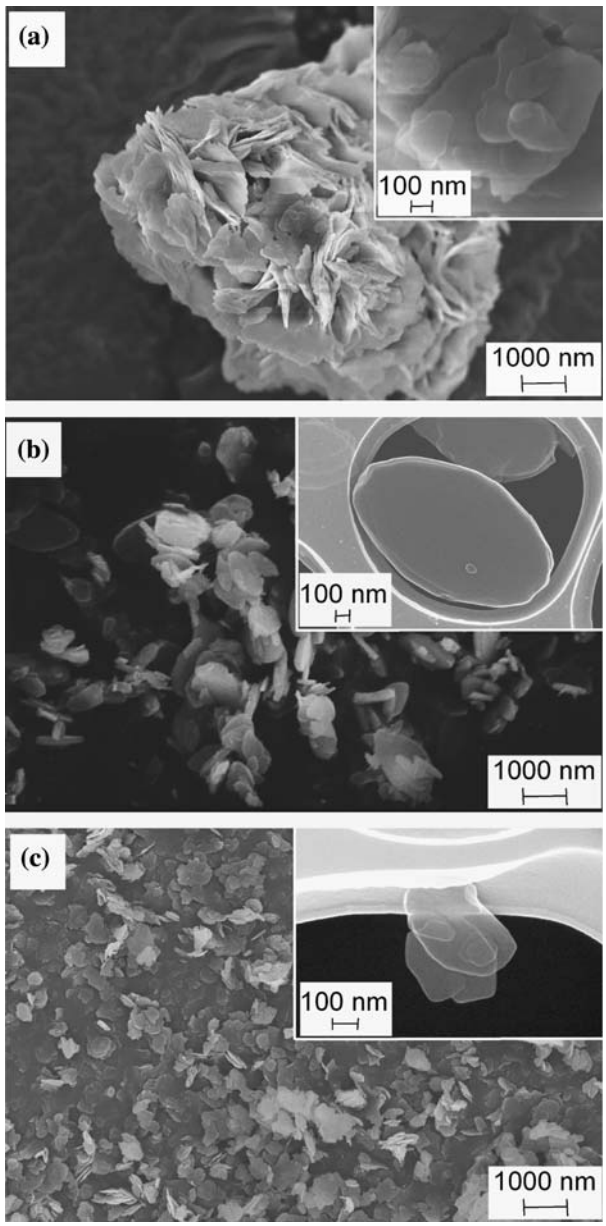

Figure 1. SEM images of precursor $VOHPO_4 \cdot 0.5H_2O$. (a) P(OSM), (b) EP(Bu), and (c) EP(Bu)-Et.

(EP(Bu)), and prepared by the organic solvent method (P(OSM)). The images show that the microstructures of these precursors are significantly different, according to the preparation method. The P(OSM) precursor was rose-petal shaped particles consisted of microcrystallites of varied sizes in the range of 100–1000 nm (figure 1a), as reported previously [17]. Crystallites of EP(Bu) exhibited a leaf-like shape with dimensions of about 1000 nm in length and 150 nm in thickness (figure 1b), in which the thickness (t; nm) was estimated by equation (1) using a density (ρ; g cm^{-3}), surface area (S; m^2 g^{-1}), and lateral length of the crystallites (L; mm) [16,17]. 1

$$\frac{2000}{t} + \frac{4}{L} = S\rho. \quad (1)$$

However, when the exfoliation-reduction of $VOPO_4 \cdot 2H_2O$ was carried out in the mixture of 2-butanol and ethanol this gave much smaller and uniform sized crystallites (EP(Bu)-Et), which was composed of nanometer-sized thin crystallites having a length of 300 nm and a thickness of 40 nm (figure 1c). The three samples were confirmed to be crystalline $VOHPO_4 \cdot 0.5H_2O$ by XRD and IR (data not shown) and monolithic particles were observed in the transmission electron microscope (TEM) images of these samples (data not shown).

The precursors were transformed into catalysts in the mixture of *n*-butane (1.5 vol%), O_2 (17 vol%), and He (balance) at 663 K for 300 h, in which the catalyst is defined as the sample giving a stationary activity and selectivity for the oxidation of *n*-butane. Figure 2 presents SEM and TEM images of catalysts derived from the precursors EP(Bu)-Et, EP(Bu), and P(OSM). The apparent shape and length of the catalyst particles derived from P(OSM) and EP(Bu) (denoted C(OSM) and EC(Bu), respectively) were similar to those of the corresponding precursors shown in the SEM images. However, the TEM images of EC(Bu) (inset in figure 2b) clearly show that the particles are polycrystalline and consist of a distinct peripheral shell and nano-sized crystallites of about 50 nm in length inside [19]. Catalyst particles of C(OSM) are also reported to be polycrystalline [20]. In contrast to these systems, catalyst particles (denoted EC(Bu)-Et) derived from EP(Bu)-Et consist of bare, sharply-angular nano-sized crystallites with rectangular shapes having sides of about 50 nm. The crystallites of EC(Bu)-Et are significantly different in shape and dimensions to the corresponding precursor. The electron diffraction pattern of EC(Bu)-Et (inset in figure 2d) gave sharp spots corresponding to the (100) plane of $(VO)_2P_2O_7$, this indicates that the nano-sized crystallites were single crystals of $(VO)_2P_2O_7$. The state of aggregation of the EC(Bu)-Et crystallites is quite different to that of EC(Bu). It should be emphasized that the nano-sized crystallites of EC(Bu)-Et are separated from each other.

The XRD patterns of C(OSM), EC(Bu), and EC(Bu)-Et showed the presence of a single phase of $(VO)_2P_2O_7$, without non-selective phases such as α_{II}-$VOPO_4$ (figure 3a). Figure 3b presents mesopore size distributions of the catalysts estimated from N_2 desorption isotherms at 77 K. A broad peak around 3–10 nm was observed for C(OSM) and an intense, sharp peak around 4 nm for EC(Bu). Since a crystallite of $(VO)_2P_2O_7$ is nonporous, these mesopores can be attributed to the voids between the nano-sized crystallites. In contrast, it is worthy of note that EC(Bu)-Et contained no mesopores, supporting the idea mentioned above that each nano-sized $(VO)_2P_2O_7$ crystallite of EC(Bu)-Et exists apart (figure 2c). Using the dimensions of the nano-sized crystallites (50 nm × 50 nm × 30 nm) and their density (3.34 g cm^{-3}), the surface area of EC(Bu)-Et was calculated to be 44 m^2 g^{-1}. This value agrees well with the surface area of 46 m^2 g^{-1} estimated by BET using the N_2 adsorption isotherm.

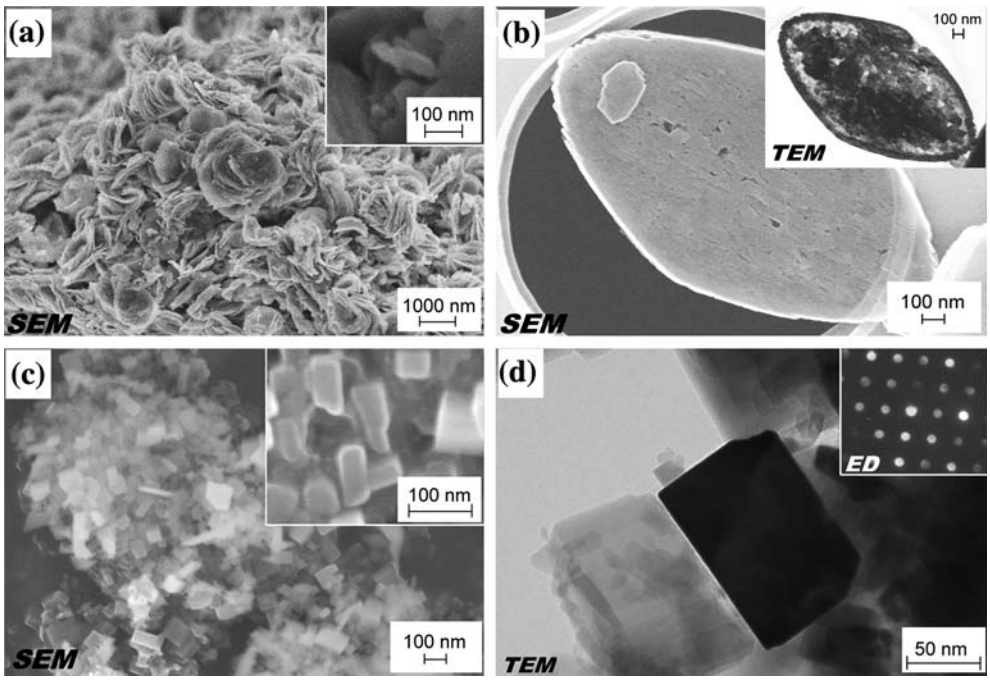

Figure 2. SEM and TEM images of the catalysts. SEM images of (a) C(OSM), (b) EC(Bu) (inset: TEM image), and (c) EC(Bu)-Et and TEM image of (d) EC(Bu)-Et (inset: electron diffraction pattern, which corresponds to the (100) plane of $(VO)_2P_2O_7$).

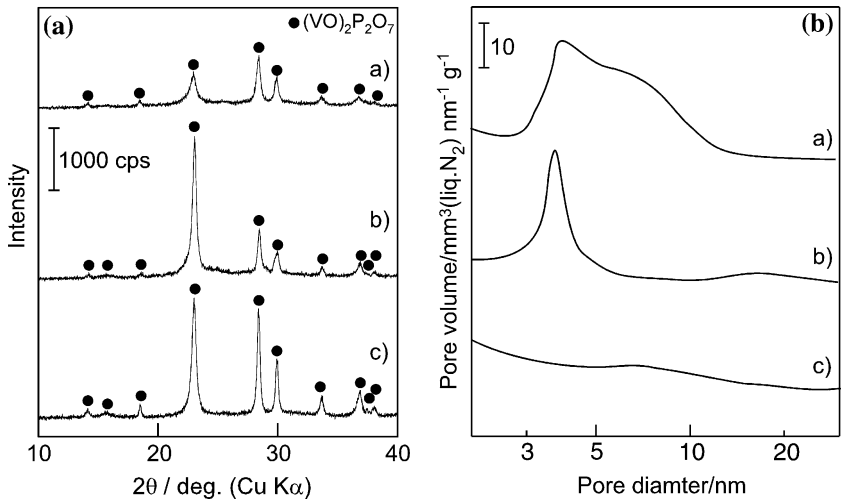

Figure 3. (a) XRD pattern and (b) pore-size distribution of the catalysts. (a) C(OSM), (b) EC(Bu), and (c) EC(Bu)-Et.

The selectivity for and yield of MA on the basis of *n*-butane are plotted against the conversion of *n*-butane (figure 4). The catalysts EC(Bu)-Et and EC(Bu), which were prepared by the exfoliation-reduction of $VOPO_4 \cdot 2H_2O$, showed a higher selectivity than the conventional C(OSM) catalyst. In particular, EC(Bu)-Et gave a remarkably high selectivity for MA, reaching about 84% at low conversion levels, and remaining at 78% even at 85% conversion. Consequently, the maximum yield of MA over EC(Bu)-Et was about 70%. Three samples of EC(Bu)-Et which were prepared separately gave nearly the same activity and selectivity. In addition, EC(Bu)-Et exhibited a high activity and the activities of the catalysts were found to be in the order of EC(Bu)-Et (49×10^{-4} mol g^{-1} h^{-1}) > C(OSM) (32×10^{-4} mol g^{-1} h^{-1}) > EC(Bu) (22×10^{-4} mol g^{-1} h^{-1}). This observation is consistent with the surface areas of the catalysts (table 1). These results demonstrate that the novel preparation of $(VO)_2P_2O_7$ reported here, comprising the exfoliation-reduction of $VOPO_4 \cdot 2H_2O$ in the mixture of 2-butanol and ethanol, gave the separate nano-sized crystallites of $(VO)_2P_2O_7$, being a highly active and selective catalyst for the oxidation of *n*-butane to MA.

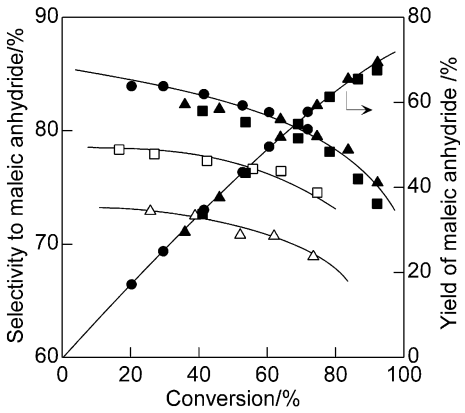

Figure 4. Results of the catalysis of the oxidation of *n*-butane over (Δ) C(OSM), (□) EC(Bu), and (●, ▲, ■) EC(Bu)-Et.

A comparison of EC(Bu)-Et and EC(Bu) shows both to have well-crystallized $(VO)_2P_2O_7$ (figure 3a) and almost the same oxidation state of V in the bulk and at the surface (table 1), indicating that the structure for both catalysts in the bulk and at the surface was basically the same. However, there is a striking difference between the state of aggregation of the nano-sized $(VO)_2P_2O_7$ crystallites which were comprised in the catalyst particles of both EC(Bu)-Et and EC(Bu). The nano-sized crystallites of EC(Bu)-Et exist apart and this lack of aggregation results in an absence of mesopores, whereas the nano-sized crystallites of EC(Bu) aggregate to form catalyst particles with mesopores. It is speculated that in the gas-phase oxidation of hydrocarbons, the further oxidation of the reactants and products to CO_2 is facilitated in the cavities of micro- and mesopores, due to the prolonged stay of the components in these pores. Therefore, the excellent selectivity of EC(Bu)-Et can be attributed to its lack of such mesopores, which is due to the characteristic shape of its nano-sized $(VO)_2P_2O_7$ crystallites. Since highly crystalline $(VO)_2P_2O_7$ shows a high selectivity for MA when compared with less crystalline $(VO)_2P_2O_7$, it can be assumed

Table 1
Physical properties of the catalysts

Catalyst	SA[a] (m^2 g^{-1})	*n* of V^{n+}	
		Bulk[b]	Surface[c]
EC(Bu)-Et	46	4.01	4.31
EC(Bu)	22	4.08	4.23
C(OSM)	23	4.07	4.31

[a]After pretreatment at 523 K in a vacuum.
[b]Average oxidation number of vanadium estimated by redox-titration.
[c]Estimated from XPS.

that the excellent, high selectivity observed for EC(Bu)-Et is due to both its highly crystalline state as well as its lack of mesopores.

Acknowledgment

This work was supported by Core Research for Evolution Science and Technology (CREST) of the Japan Science and Technology Corporation (JST).

Reference

[1] G. Centi, F. Trifirò, J.R. Ebner and V.M. Franchetti, Chem. Rev. 88 (1988) 55.
[2] G. Centi, F. Cavani and F. Trifirò, in: *Selective Oxidation by Heterogeneous Catalysis*, (Kluwer Academic, New York, 2001), p. 143 .
[3] G.J. Hutchings, J. Mater. Chem. 14 (2004) 3385.
[4] T. Okuhara, K. Inumaru and M. Misono, Chem. Lett. (1992) 1955.
[5] E. Bordes, Catal. Today 16 (1993) 27.
[6] P.A. Agaskar, L. DeCaul and R.K. Grasselli, Catal. Lett. 23 (1994) 339.
[7] A. Takagi, M. Sugisawa, D. Lu, J.N. Kondo, M. Hara, K. Domen and S. Hayashi, J. Am. Chem. Soc. 125 (2003) 5479.
[8] R. Abe, S. Ikeda, J.N. Kondo, M. Hara and K. Domen, Thin Solid Films 343 (1999) 156.
[9] P.J. Ollivier, N.I. Kovtyukhova, S.W. Keller and T.M. Mallouk, Chem. Commun. (1998) 1563.
[10] S.W. Keller, H.-N. Kim and T.E. Mallouk, J. Am. Chem. Soc. 116 (1994) 8817.
[11] G. Alberti, S. Cavalaglio, F. Marmottini, K. Matusek, J. Megyeri and L. Szirtes, Appl. Catal. A 218 (2001) 219.
[12] R. Abe, K. Shinohara, A. Tanaka, M. Hara, J.N. Kondo and K. Domen, Chem. Mater. 10 (1998) 329.
[13] H. Nakajima and G. Matsubayashi, J. Mater. Chem. 5 (1995) 105.
[14] L. Berebš, J. Votinsky, J. Kalousová and J. Klikorka, Inorg. Chim. Acta 114 (1986) 47.
[15] L. Beneš, J. Votinsky, J. Kalousová and K. Handlí, Inorg. Chim. Acta 176 (1990) 255.
[16] N. Yamamoto, N. Hiyoshi and T. Okuhara, Chem. Mater. 14 (2002) 3882.
[17] N. Hiyoshi, N. Yamamoto, N. Ryumon, Y. Kamiya and T. Okuhara, J. Catal. 221 (2004) 225.
[18] H. Igarashi, K. Tsuji, T. Okuhara and M. Misono, J. Phys. Chem. 97 (1993) 7065.
[19] Y. Kamiya, N. Hiyoshi, N. Ryumon and T. Okuhara, J. Mol. Catal. A 220 (2004) 103.
[20] C.J. Kiely, A. Burrows, G.J. Hutchings, K.E. Bere, J.-C. Volta, A. Tuel and M. Abon, Faraday Discuss. 105 (1996) 103.